

# Anti-sway control method for crane obstacle avoidance

Ngo Van An

Thai Nguyen University of Technology

## Abstract

Overhead cranes are increasingly being utilized in various industries for material transportation. However, issues related to the natural oscillation of loads affect both the safety and efficiency of transportation. Additionally, in certain scenarios where the crane operates in spaces with obstacles, there is a need for a control method that minimizes load oscillation and avoids obstacles, thereby ensuring operational safety and efficiency. This paper presents a dynamic model of the overhead crane as a foundation for further research. It proposes an extended PD control law to mitigate oscillations and enhance the safety of crane operations. The paper also includes simulations demonstrating the impact of controller parameters on the crane's performance. Finally, it introduces the concept of a control method aimed at obstacle avoidance.

**Keywords:** overhead crane, swing angle, over-adjustment, obstacle avoidance

Date of Submission: 09-05-2024

Date of acceptance: 21-05-2024

## Symbol

Symbol	Unit	Meaning
$H, C, F, G$		Matrices of dynamic equations
$m_r, m_c, m_p$	Kg	are the mass of the rig, the car and the load, respectively.
J	$kg.m^2$	is the moment of inertia of the system.
G	$m/s^2$	is the gravitational acceleration.
$f_x, f_y$	N	is the force acting on the system in the X and Y directions along the force trajectory f
L	M	Length of wire connecting crane and load.

## I. Introduction

Overhead cranes are widely utilized lifting devices in workshops, factories, and seaports, aiding in the lifting and transporting of large and heavy goods, thus reducing manual labor and enhancing productivity. Primarily powered by electric motors, overhead cranes find extensive use in industrial plants, steel mills, hydropower stations, and civil applications. Given their operation in harsh conditions such as dusty, hazardous, and dangerous environments, the role of overhead cranes is crucial for production activities and occupational safety. Consequently, effective and high-efficiency crane control is of significant interest. Various studies have explored control methods for overhead cranes, including classical PD control and energy square control [1]. While these methods are computationally light, their control quality is often suboptimal. Other research has employed fuzzy control, neural networks, or adaptive control [6-8]. These methods improve control quality but are computationally intensive and complex. Among the considered approaches, the extended PD controller strikes a balance with manageable computational load and control parameters, yet delivers high-quality control results, short transient times, high precision, and robustness against system uncertainties.

During operation, obstacles may appear within the crane's working space, which previous methods have not addressed in terms of obstacle avoidance. According to [9], some consideration has been given to obstacle avoidance, but it assumed linear and independent crane motion components during design. This paper examines an extended PD controller [5] to control a nonlinear crane model to reduce oscillations and incorporates trajectory design methods to avoid obstacles within the operational space.

The content of this paper includes the following sections: Crane modeling, presentation of the extended PD algorithm and evaluation of the impact of controller parameters on control quality, explanation of the obstacle avoidance trajectory design algorithm, and using the designed avoidance trajectory as the target trajectory for the crane with the extended PD controller. Finally, observations and conclusions are provided.

## II. Crane modeling

The crane model is considered with the coordinate system OXYZ as shown in Figure 1, where the gantry moves along the OX axis, the trolley moves along the OY axis, and the load moves along the OZ axis. The angles representing load oscillations,  $\theta$  and  $\phi$ , are determined as depicted in the figure. In the scope of this research, we consider the case where  $L$  remains constant during system operation, meaning that in practice, the load is lifted and lowered before and after controlling the crane.

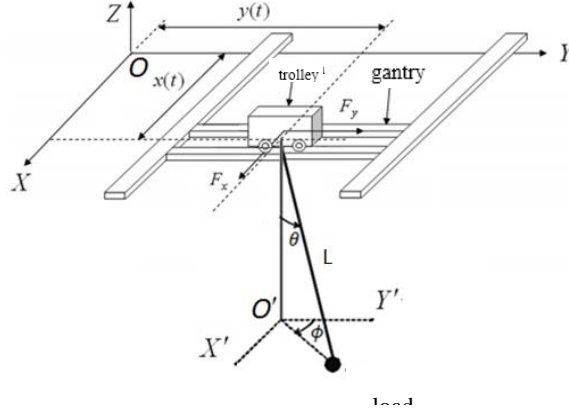


Figure 1: Crane model

Using the Lagrange equation, we can build the dynamic equation of the bridge crane as follows [1]:

$$\mathbf{H}(\mathbf{q})\ddot{\mathbf{q}} + \mathbf{C}(\mathbf{q}, \dot{\mathbf{q}})\dot{\mathbf{q}} + \mathbf{G}(\mathbf{q}) = \mathbf{F} \quad (1)$$

In which:

$$\mathbf{q} = \begin{bmatrix} x \\ y \\ \theta \\ \phi \end{bmatrix}; \quad \mathbf{F} = \begin{bmatrix} f_x \\ f_y \\ 0 \\ 0 \end{bmatrix}; \quad \mathbf{G}(\mathbf{q}) = \begin{bmatrix} 0 \\ 0 \\ G_{31} \\ 0 \end{bmatrix}; \quad \mathbf{H}(\mathbf{q}) = \begin{bmatrix} H_{11} & 0 & H_{13} & H_{14} \\ 0 & H_{22} & H_{23} & H_{24} \\ H_{31} & H_{32} & H_{33} & 0 \\ H_{41} & H_{42} & 0 & H_{44} \end{bmatrix}; \quad \mathbf{C}(\mathbf{q}, \dot{\mathbf{q}}) = \begin{bmatrix} 0 & 0 & C_{13} & C_{14} \\ 0 & 0 & C_{23} & C_{24} \\ 0 & 0 & 0 & C_{34} \\ 0 & 0 & C_{43} & C_{44} \end{bmatrix}$$

$$H_{11} = m_p + m_c + m_r$$

$$H_{13} = m_p \cdot L \cdot \cos \theta \cdot \sin \phi$$

$$H_{14} = m_p \cdot L \cdot \sin \theta \cdot \cos \phi$$

$$H_{22} = m_p + m_c \quad H_{23} = m_p \cdot L \cdot \cos \theta \cdot \cos \phi$$

$$H_{24} = -m_p \cdot L \cdot \sin \theta \cdot \sin \phi$$

$$H_{31} = m_p \cdot L \cdot \cos \theta \cdot \sin \phi \quad H_{32} = m_p \cdot L \cdot \cos \theta \cdot \cos \phi$$

$$H_{33} = m_p \cdot L^2 + J$$

$$H_{41} = m_p \cdot L \cdot \sin \theta \cdot \cos \phi$$

$$H_{42} = -m_p \cdot L \cdot \sin \theta \cdot \sin \phi$$

$$H_{44} = m_p \cdot L^2 \cdot \sin^2 \theta + J$$

$$C_{13} = -m_p \cdot L \cdot \sin \theta \cdot \sin \phi \cdot \dot{\theta} + m_p \cdot L \cdot \cos \theta \cdot \cos \phi \cdot \dot{\phi}$$

$$C_{14} = m_p \cdot L \cdot \cos \theta \cdot \cos \phi \cdot \dot{\theta} - m_p \cdot L \cdot \sin \theta \cdot \sin \phi \cdot \dot{\phi}$$

$$C_{23} = -m_p \cdot L \cdot \sin \theta \cdot \cos \phi \cdot \dot{\theta} - m_p \cdot L \cdot \cos \theta \cdot \sin \phi \cdot \dot{\phi}$$

$$C_{24} = -m_p \cdot L \cdot \cos \theta \cdot \sin \phi \cdot \dot{\theta} - m_p \cdot L \cdot \sin \theta \cdot \cos \phi \cdot \dot{\phi}$$

$$C_{34} = -m_p \cdot L^2 \cdot \sin \theta \cdot \cos \theta \cdot \dot{\phi}; \quad C_{43} = m_p \cdot L^2 \cdot \sin \theta \cdot \cos \theta \cdot \dot{\phi}$$

$$C_{44} = m_p \cdot L^2 \cdot \sin \theta \cdot \cos \theta \cdot \dot{\theta}$$

$$G_{31} = m_p \cdot g \cdot L \cdot \sin \theta$$

From (1) we have:

$$\ddot{\mathbf{q}} = \mathbf{H}(\mathbf{q})^{-1} \cdot (\mathbf{F} - \mathbf{C}(\mathbf{q}, \dot{\mathbf{q}})\dot{\mathbf{q}} - \mathbf{G}(\mathbf{q})) \quad (2)$$

Put :

$$\ddot{\mathbf{r}} = \frac{1}{\det(\mathbf{H})} \cdot (\mathbf{P}\mathbf{f} + \mathbf{W}) \quad (3)$$

In which:

$$\mathbf{r} = \begin{bmatrix} x \\ y \end{bmatrix}; \quad \mathbf{P} = \begin{bmatrix} P_{11} & P_{12} \\ P_{21} & P_{22} \end{bmatrix}; \quad \mathbf{W} = \begin{bmatrix} W_1 \\ W_2 \end{bmatrix}; \quad \mathbf{f} = \begin{bmatrix} f_x \\ f_y \end{bmatrix}$$

$$P_{11} = H_{22} \cdot H_{33} \cdot H_{44} - H_{23} \cdot H_{32} \cdot H_{44} - H_{24} \cdot H_{33} \cdot H_{42}$$

$$P_{12} = H_{13} \cdot H_{32} \cdot H_{44} + H_{14} \cdot H_{33} \cdot H_{42}$$

$$P_{21} = H_{23} \cdot H_{31} \cdot H_{44} + H_{24} \cdot H_{33} \cdot H_{41}$$

$$P_{22} = H_{11} \cdot H_{33} \cdot H_{44} - H_{13} \cdot H_{31} \cdot H_{44} - H_{14} \cdot H_{33} \cdot H_{41}$$

$$W_1 = -P_{11} \cdot V_{11} - P_{12} \cdot V_{21} - (-H_{22} \cdot H_{13} \cdot H_{44} + H_{13} \cdot H_{42} \cdot H_{24} - H_{14} \cdot H_{23} \cdot H_{42}) \cdot (V_{31} + G_{31})$$

$$-(-H_{32} \cdot H_{13} \cdot H_{24} - H_{14} \cdot H_{22} \cdot H_{33} + H_{14} \cdot H_{23} \cdot H_{32}) \cdot V_{41}$$

$$W_2 = -P_{21} \cdot V_{11} - P_{22} \cdot V_{21} - (-H_{11} \cdot H_{23} \cdot H_{44} - H_{13} \cdot H_{41} \cdot H_{24} + H_{14} \cdot H_{23} \cdot H_{41}) \cdot (V_{31} + G_{31})$$

$$-(-H_{11} \cdot H_{33} \cdot H_{24} + H_{13} \cdot H_{31} \cdot H_{24} - H_{14} \cdot H_{23} \cdot H_{31}) \cdot V_{41}$$

### 3. Control algorithm

The purpose of building a control algorithm is to control the crane to the desired position, and at the same time the angle of deviation of the load from the vertical converges to 0.

Setting  $\boldsymbol{\varepsilon} = \mathbf{r} - \mathbf{r}_d = [x - x_d \quad y - y_d]^T = [x_e \quad y_e]^T$  with  $\mathbf{r}_d$  is the position of the crane truck. According to [5] we have an extended PD controller:

$$\mathbf{F} = \left( \frac{\mathbf{P}}{\det(\mathbf{H})} \right)^{-1} \cdot \left( -k_\varepsilon^2 \cdot \boldsymbol{\varepsilon} - 2k_\varepsilon \cdot \dot{\boldsymbol{\varepsilon}} - \frac{\mathbf{W}}{\det(\mathbf{H})} + \ddot{\mathbf{r}}_d + \begin{bmatrix} \sin \phi \\ \cos \phi \end{bmatrix} \cdot \mathbf{f} \right)$$

Where  $k_\varepsilon$  is a positive constant,  $\mathbf{f}$  determined by:

$$\mathbf{f} = \left\{ \kappa[k_\theta \cdot \theta + 2\dot{\theta}] + (k_\theta \cdot \theta + 2\dot{\theta}) \cdot (\sin^2 \theta + k_\theta \cdot \theta^2) \right\} \cdot / \sin \phi \cdot (-\dot{x}_d + 2k_\varepsilon \cdot \dot{x}_e + k_\varepsilon^2 \cdot x_e) + \cos \phi \cdot (-\dot{y}_d + 2k_\varepsilon \cdot \dot{y}_e + k_\varepsilon^2 \cdot y_e) + \kappa[k_\theta \cdot \theta + 2\dot{\theta}] \cdot \left| \frac{k_\theta \cdot \theta}{\sqrt{\bar{a}}} \right| + (k_\theta \cdot \theta + 2\dot{\theta}) + L \cdot \sin \theta \cdot \dot{\phi}^2$$

$$\bar{a} = \left( \frac{m_p \cdot L \cdot \cos \theta}{m_p \cdot L^2 + J} \right)^2$$

Where:  $k_\theta$  is a positive coefficient,

$\kappa(\mathbf{x})$  is the function defined:

$$\kappa(\mathbf{x}) = \begin{cases} \text{sgn}(\mathbf{x}) & n\tilde{\omega} |\mathbf{x}| \geq \gamma(t) \\ \sin\left(\frac{\mathbf{x}}{\gamma(t)} \cdot \frac{\pi}{2}\right) & n\tilde{\omega} |\mathbf{x}| < \gamma(t) \end{cases}$$

The function  $\gamma(t)$  is defined by:  $\gamma(t) = \frac{1}{\alpha + \beta \cdot e^{\eta \cdot t}}$ ;

Where  $\alpha, \beta, \eta$  are the coefficients,  $0 \leq \gamma(t) \leq \varepsilon \ll 1, t \geq 0$

Controller parameters:  $\alpha, \beta, \eta, k_\theta, k_e$

Proving the stability and sustainability of the controller can be seen in detail in [5].

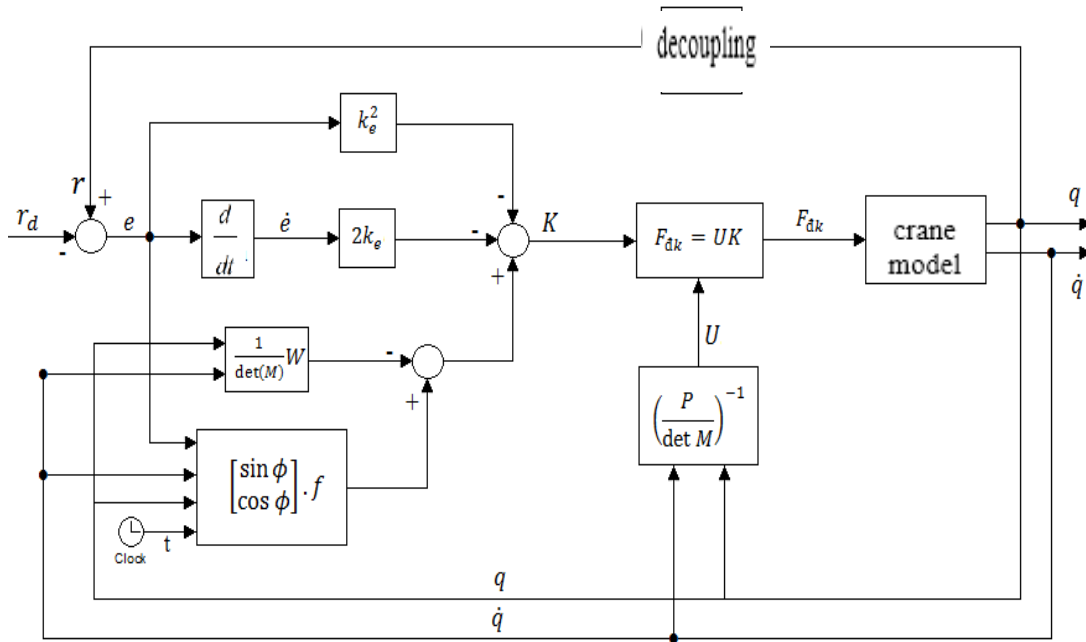


Figure 2: Expanded PD control block diagram

One of the key issues in utilizing controllers is the selection of control parameters. To make a reasonable selection, this paper evaluates the impact of control parameters on system performance. Among the control parameters,  $\beta$  and  $k_e$  have the most significant influence on control quality. Therefore, this paper will simulate and assess the impact of these two parameters on control quality.

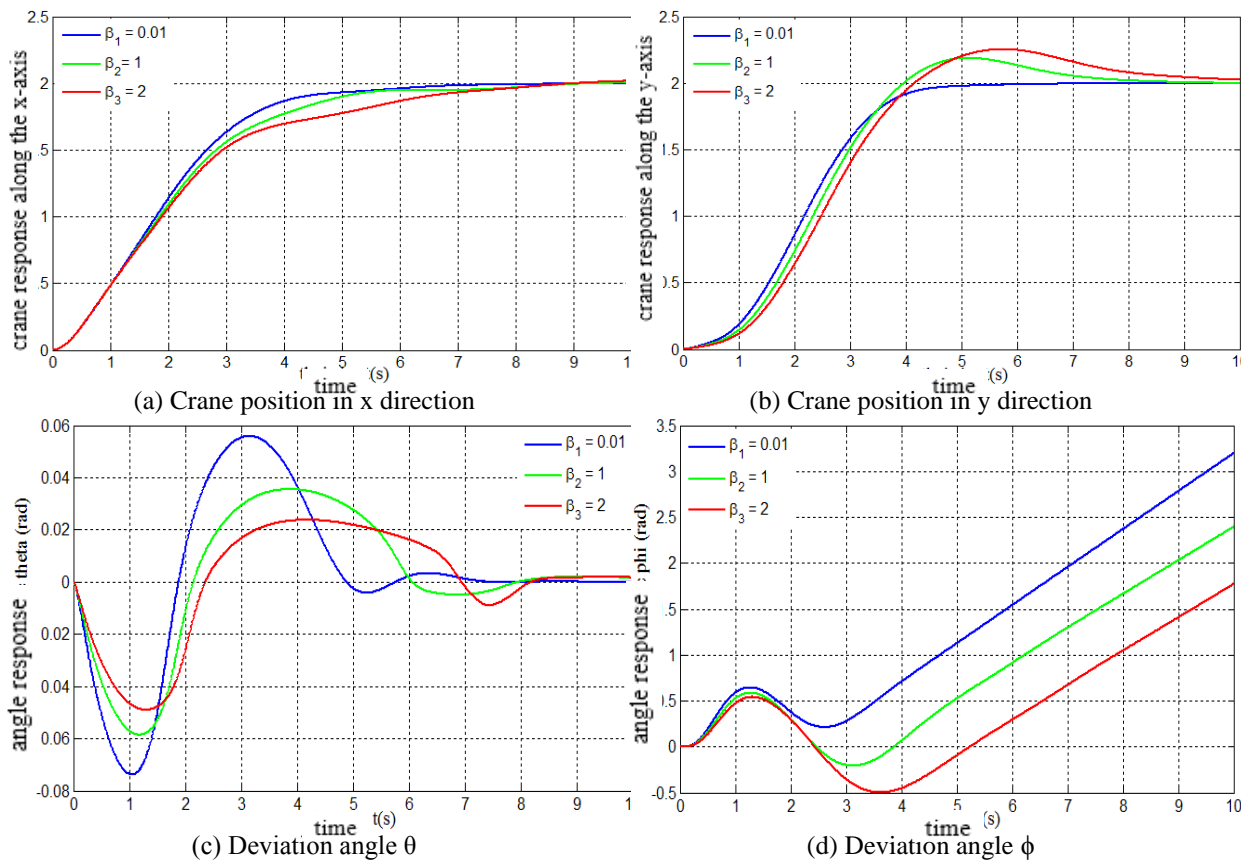
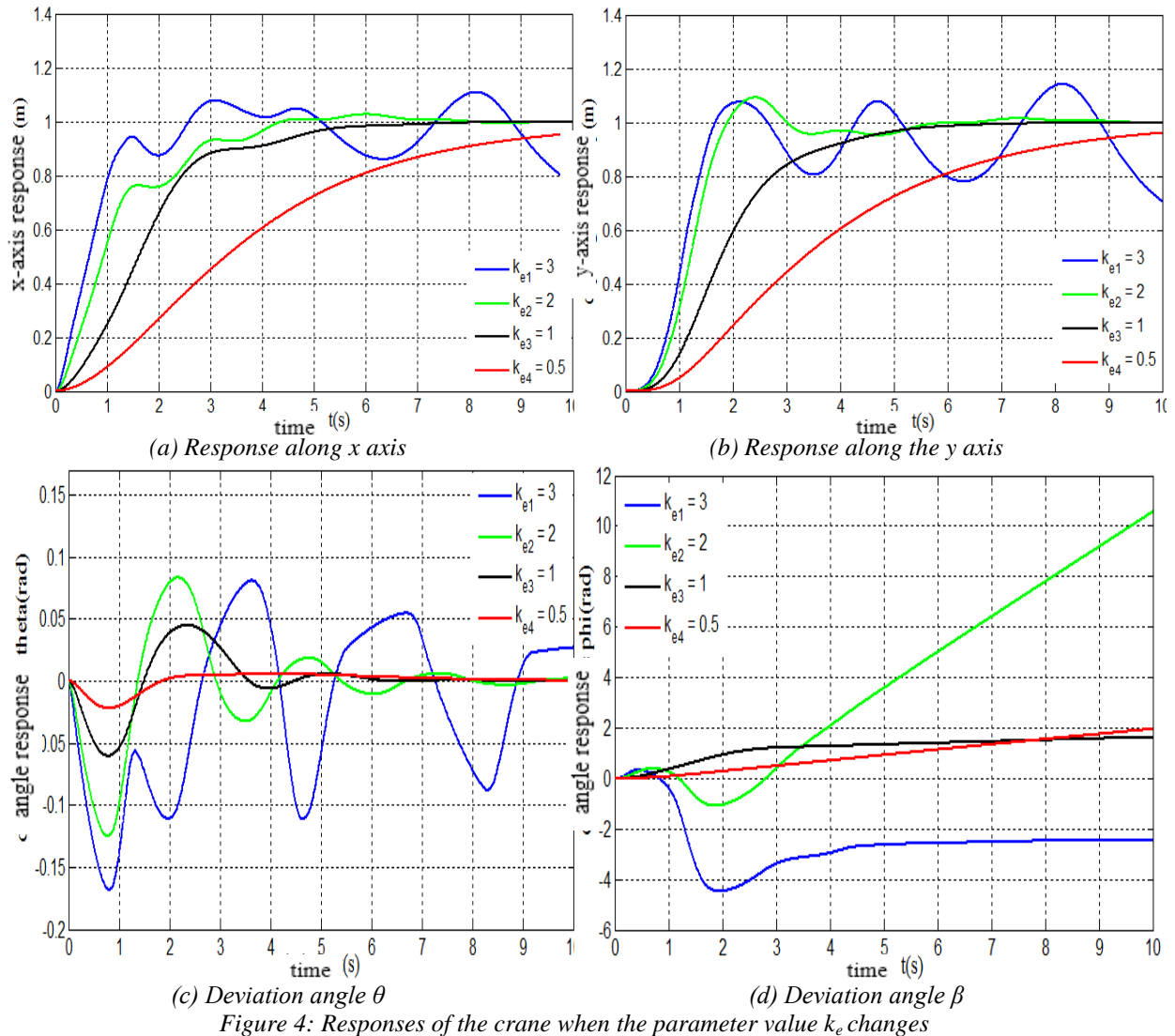


Figure 3: Crane responses when parameter  $\beta$  changes



Figures 3 and 4 illustrate the crane's response to variations in parameters  $\beta$  và  $k_e$ . It can be observed that changes in these parameters affect all state variables of the crane.

The control parameters  $\beta$  và  $k_e$  greatly influence the system's stability, especially parameter  $k_e$ . When parameter  $b$  is adjusted to a high value ( $b = 2$ ), it causes overshoot in position control and increases the oscillation duration of angle  $\theta$ . However, when parameter  $b$  is gradually reduced (towards 0), the system operates stably and as required (shorter oscillation duration of angle  $\theta$ ) without overshoot. Therefore,  $b$  should be adjusted within the range of 0 to 0.2.

The control parameter  $k_e$  significantly affects the stability of the crane's operation. When  $k_e = 3$ , the crane operates unstably but with a short transient time ( $t \approx 2s$ ). Only when  $k_e$  is reduced does the crane operate stably. As  $k_e$  is further reduced, the amplitude and duration of crane oscillations decrease, but the transient time increases. Thus,  $k_e$  should be adjusted within the range of 0.5 to 1.5.

### III. Obstacle avoidance control for cranes

During crane operations, obstacles may appear in the working space. Therefore, it is crucial to address this issue with appropriate methods and algorithms to control the crane in order to avoid obstacles. Within the scope of this study, we consider the case where the position and shape of the obstacles are known in advance.

To control the crane to avoid obstacles, we will develop an obstacle avoidance trajectory and use this trajectory as the reference signal for the system with anti-sway control. Since directly controlling the load is relatively difficult, we will control the load indirectly by controlling the crane's trolley.

time

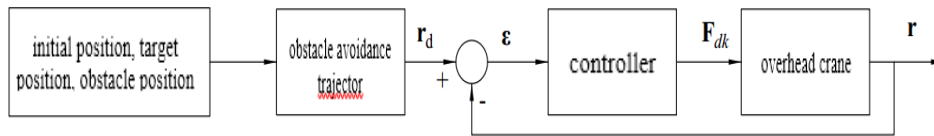


Figure 5: Block diagram of crane control to avoid obstacles

Next we will proceed to build a trajectory to avoid obstacles:

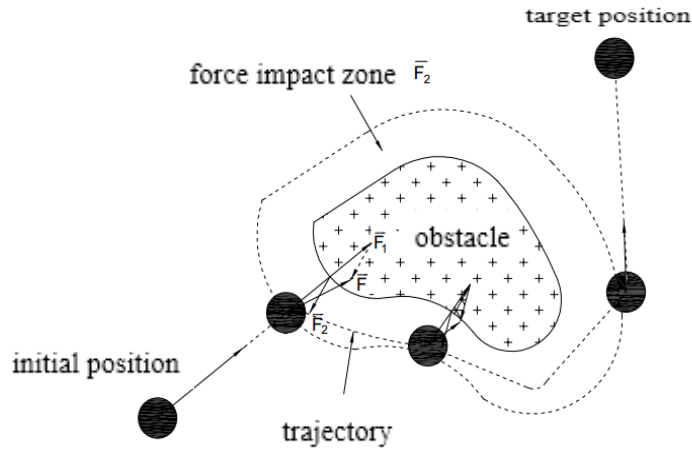


Figure 6: Drawing depicting the obstacle avoidance method

To control the crane to avoid obstacles, we will apply a force to the crane  $\vec{F}$

$$\vec{F} = \vec{F}_1 + \vec{F}_2$$

In which :  $\vec{F}_1$  is the force pulling the crane to its set position

$\vec{F}_2$  is the force to push the crane away from the obstacle

We choose the function  $\vec{F}_1$  takes the form of a PD controller:

$$\vec{F}_1 = -k_p \cdot (\mathbf{r} - \mathbf{r}_d) - k_v \cdot \dot{\mathbf{r}}$$

In which :  $k_p, k_v$  is a positive coefficient

$\mathbf{r}$  is the current position vector

$\mathbf{r}_d$  is the set position vector (destination position)

$\dot{\mathbf{r}}$  is the velocity vector

$$\vec{F}_2 = \begin{cases} 0 & \text{when } \rho > \rho_0 \\ \eta \left( \frac{1}{\rho} - \frac{1}{\rho_0} \right) \frac{1}{\rho^2} \frac{\partial \rho}{\partial \mathbf{r}} & \text{when } \rho \leq \rho_0 \end{cases}$$

The choice of function  $\vec{F}_2$  has the following form:

In which:  $\rho$  is the distance between the crane and the obstacle

$\rho_0$  is the distance of the area affected by the obstacle and  $\rho_0$  is a constant

$$\eta \text{ is a constant } \frac{\partial \rho}{\partial \mathbf{r}} = \left[ \frac{\partial \rho}{\partial x} \quad \frac{\partial \rho}{\partial y} \right]^T$$

Simulation results:

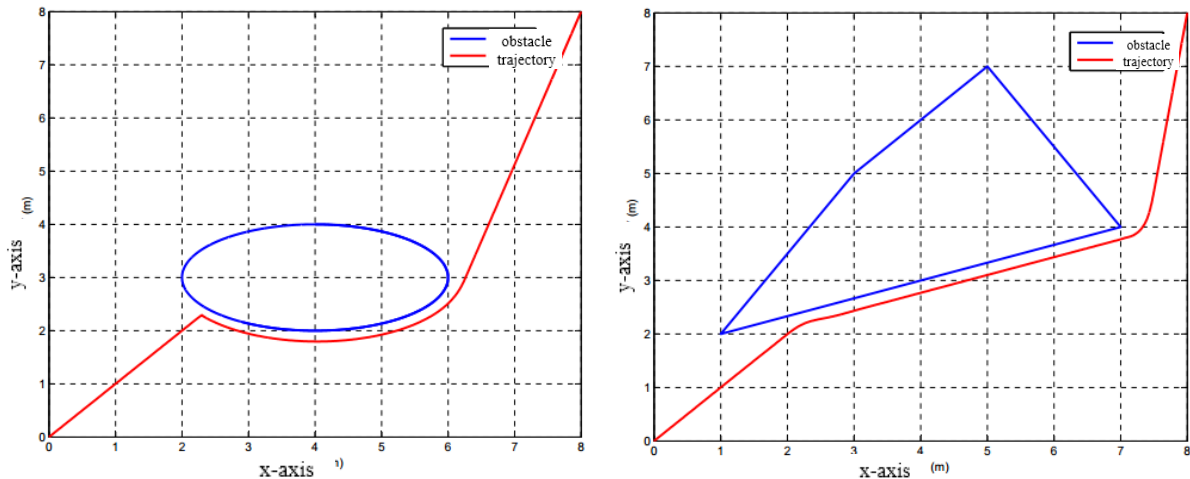


Figure 7: Obstacle avoidance trajectory for some types of obstacles

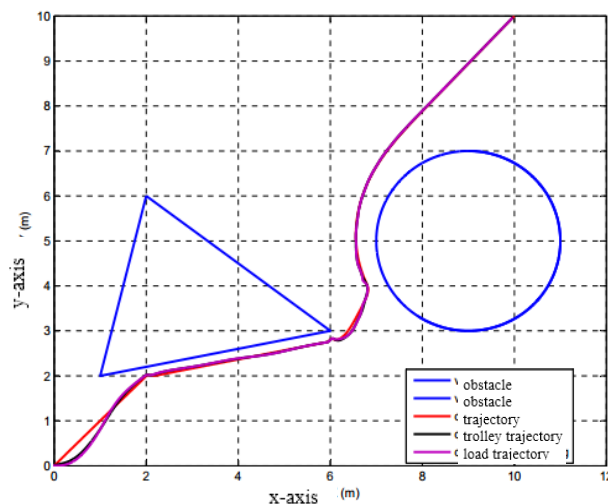


Figure 8: Response of the crane when avoiding obstacles

Figure 3 and Figure 4 show the system response to corresponding changes in parameters

The trajectory we construct, according to theoretical principles (Figure 6), meets the requirements of obstacle avoidance  $\rho_0$  and maintains a specified distance from the obstacles. The trajectory is smooth and continuous.

From Figure 8, it can be observed that when simulating the crane following the pre-set trajectory, the crane successfully avoids the obstacles. The trajectories of both the trolley and the load follow the reference trajectory. These two trajectories are nearly indistinguishable due to the position control and anti-sway functionality of the extended PD controller. This indicates that the crane system effectively mitigates sway while moving to avoid obstacles. At the initial moments and when the reference trajectory changes direction, there is a lag between the trajectories of the trolley and the load relative to the reference trajectory. This lag is due to the system's inertia, a phenomenon not addressed within the scope of this paper.

### References

- [1]. Y. Fang, W. E. Dixon, E. Zergeroglu, and D. M. Dawson, "Nonlinear coupling control laws for a 3-DOF overhead crane system", Proceedings of 40<sup>th</sup> IEEE Conference on Decision and Control, Orlando, Florida USA, December 2001, pp. 3776-3771.
- [2]. Oussama Khatib, "Real-Time Obstacle Avoidance for Manipulator and Mobile Robots", The International Journal of Robotics Research, Vol.5, No.1, Spring 1986, pp. 90-98.
- [3]. Y. Fang, E. Zergeroglu, W. E. Dixon, and D. M. Dawson, "Nonlinear Coupling Control Laws for an Underactuated Overhead Crane System", IEEE/ASME Transactions on Mechatronics, Vol. 8, No. 3, September 2003, pp. 418-423.
- [4]. R. M. T. Raja Ismail, M. A. Ahmad, M. S. Ramli, F. R. M. Rashidi, "Nonlinear Dynamic Modelling and Analysis of a 3-D Overhead Gantry Crane System with System Parameters Variation", IJSSST, Vol. 11, No. 2, pp. 9-16.
- [5]. Dongkyoung Chwa, "Nonlinear Tracking Control of 3-D Overhead Cranes Against the Initial Swing Angle and the Variation of Payload Weight", IEEE Transactions on Control Systems Technology, Vol. 17, No. 4, July 2009, pp. 876-883.
- [6]. Dragan AntićZoran, Jovanović, Staniša Perić, Saša Nikolić, Marko Milojković, Miloš Milošević, "Anti-Swing Fuzzy Controller Applied in a 3D Crane System", IEEE Transactions on Industrial Electronics, VOL.55, NO.11, November 2008

- [7]. Belkheir BENHELLAL, Mustapha Hamerlain, Rachid Ouiguini, Yacine Rahmani “Decoupled Adaptive Neuro-Fuzzy Sliding Mode Control Applied in a 3D Crane System”, Journal of Electrical Engineering, 2014
- [8]. Yang, Jung Hua, “On the Adaptive Tracking Control of 3-D Overhead Crane Systems”,
- [9]. Akihiro KANESHIGE, Yudai KAWASAKI and Satoshi UEKI, Shunsuke NAGAI, “Development of an Autonomous Mobile Overhead Traveling Crane with on-line Obstacle Recognition and Path-Planning Based on Obstacle Information-The Design of a Transfer Control System in Consideration of Oscillating Control-“ 2<sup>nd</sup> International Symposium on Computer, Communication, Control and Automation (3CA 2013)
- [10]. Hassan K. Khalil, Nonlinear System, 3<sup>rd</sup> Edition, Prentice Hall, 2002.
- [11]. R. Lozano, I.Fantoni, and D. J. Block, “Stabilization of the inverted pendulum around its homoclinic orbit”, Systems & Control Letters, vol. 40, pp. 197–204, 2000.
- [12]. Nguyen Manh Tien, Industrial Robot Control, Hanoi Science and Technology Publishing House, 2007.
- [13]. Nguyen Phung Quang, Matlab & Simulink for automatic control engineers, Hanoi Science and Technology Publishing House, 2004.